Supplementary Material for "Long γ-ray bursts and core-collapse supernovae have different environments"

1 Supplementary Methods

Astrometry and the Morphology Independent Technique: If GRBs are associated with massive stars, then we might expect their locations to be correlated with the blue light of their hosts – such a correlation has long been hypothesized for SNe, and as we show in the associated paper this is a good representation of their distribution. Traditionally, studying the correlation with the light of the galaxy has been done by determining the offset of the object from the center, or centroid of the galaxy's light and comparing this with the half-light radius of the galaxy. High redshift galaxies, however, frequently have an irregular morphology. As a result the centroid of a galaxy's light may be an area of relatively low surface brightness. Thus if the GRBs are strictly correlated with the light, the standard technique would overpredict the number of bursts at the galaxy centroid, and underpredict those on outlying brighter regions. Our technique avoids this bias.

In general, if one were to use the light of the galaxy as a surrogate probability distribution for the location of the objects, one would want to take a very high resolution image of the host and convolve the image with the error distribution of a given object's astrometry. However, in cases where we rely entirely on *HST* astrometry, we can typically determine the position of the object to a small fraction of a pixel or about $\sim 0\farcs01$, but our best *HST* images only have a FWHM of $0\farcs07$. In many cases then, the true light distribution of the host has already been convolved

by a distribution wider than the astrometric error distribution. No further convolution is required. Where the astrometry relies on early ground-based images, the error distribution is sometimes larger than the FWHM of the image and a further convolution must be done to obtain an accurate representation of the probability distribution based on the light. We have limited ourselves to objects with error distributions with a FWHM of $\leq 0\farcs15$, which is comparable to or less than the scale size of the very smallest galaxies. This is also, coincidentally, roughly the resolution of the original *Hubble* Deep Field. In cases where the error of the position on the host is larger than this cutoff, we use only the GRB host magnitude and size for comparison with SN sample (all SNe in this sample have *HST* astrometry).

In our implementation the host galaxies are detected using the software package SExtractor[1]. A Gaussian filter with width three pixels was applied to the "drizzled"[2] *HST* images. A S/N cutoff of one with a minimum detection region of five pixels was used. In cases where the error in the astromety was larger than the PSF, the extracted image of the galaxy was then convolved with a Gaussian to bring the resolution of the image to the error of the astrometry. The pixels of the extracted (and in some cases convolved) host were next sorted from lowest to highest in surface brightness. We then locate the pixel on which the GRB or SN occurred and ascertain the fraction of the total light in the galaxy contained in pixels of surface brightness lower than or equal to the pixel containing the GRB or SN.

To insure that there is minimal contamination of the galaxy image by light from the transient source, where possible we have used images of the SN hosts taken before the outburst. This is

clearly not possible for the GRB hosts. However, for all GRBs and the remaining SNe we have used images taken at a sufficiently late time that any afterglow or SN is either below the noise or less than 10% of the remaining surface brightness of the host. To do this estimation for the GRBs, in cases where a redshift is known we have used a conservative estimate of the early time decay plus an additional component equal to one of the brightest SN associated with a GRB, SN 1998bw. Where no redshift was available, we have used a conservative extrapolation of early time decay. In nearly all cases this condition was easily met. In those cases where it was not, the object was not used for fractional light determination. We chose the cutoff value of 10% of the remaining surface brightness as it was found that an error of this magnitude generally had little effect on the fractional location of the burst. In particular, the reader may note that the GRBs differ from the predicted light distribution because they are highly bunched at the very brightest pixels. However it is near the median pixel, not the brightest pixel, where a small change in brightness may make a relatively larger change in the fractional position on the host.

We cannot detect all of the light of the hosts in their fainter outer regions. However, the missing fraction of light is generally small and, to the extent it is noticeable, will bias our result towards finding objects on pixels lower in fractional light than they actually are (and thus in the opposite sense of the surprising result found for the locations of GRBs). We have nonetheless attempted to check for any bias by adding noise to our images – and thus causing SExtractor to lose even more of the outer regions of the galaxies. We have increased the noise in the images by a magnitude (and thus a pixel must be a magnitude brighter to be detected). Although placing additional noise in the images leads to the non-detection of the three faintest host galaxies (GRBs

980326, 990510 and 000301C), the significance of our result regarding the positions of the objects remained unaffected.

In addition we tested changing the SExtractor significance cut by a magnitude on an early subset of the data. No significant change was found in our results. Furthermore, it should be noted that the effective cut strongly varies across the sample due to $(1 + z)^4$ cosmological dimming – particularly for the GRB sample which has a wide redshift range (though again note that we restrict this range when comparing the GRB and SN host magnitudes and sizes). The effect of cosmological dimming is again in the opposite sense of the results reported here. Finally, as an additional check, we have divided the GRB sample into low and high redshift ranges and find no significant difference in the position of the GRB on the host between the two subsets.

Host Parameters: The host galaxy sizes and magnitudes were also determined using the SExtractor software. Host galaxy sizes reported are the radius estimated by Sextractor to contain 80% of the host light. The experience of the GOODS group has shown this to be a robust estimator; however, use of the Sextractor measurement of the semi-major axis results in similarly incompatible GRB and SNe size distributions. Host magnitudes correspond to "mag-auto", determined by Sextractor, which is the program's best estimate of the entire light of the host.

Pixelization Bias: In assigning a GRB or SN a fractional position on the light of its host, we determine the fraction of light in all pixels fainter than or equal to the pixel that contains the object. This assigns all of the light in the pixel containing the object as if all the light in that pixel had a surface brightness lower than the point directly under the object. However, we do not know

the true surface brightness distribution of light interior to this pixel. Therefore this method assigns some light in the pixel which truly lies above that underlying the object to the total light equal to or less than that under the object. Thus there is a bias equal to some fraction of the light in the pixel containing the object. As there are typically hundreds of pixels in a host, this bias is usually, but not always, only a fraction of a percent of the host light.

Although a complete correction of this bias would require knowledge of the light distribution in the pixel containing the object (or perhaps an attempt at deconvolution on a finer pixel grid), as a first estimate one might assume that typically one-half the light of the pixel lay below the surface brightness at the location of the object and one-half above this surface brightness.

Using the half-light estimate instead of the entire pixel, however, does not noticeably change any of our results. The K-S significance is determined by the maximum vertical separation between the sample histogram and a model or a comparison sample histogram. In this case that maximum distance is effectively determined by the location of GRB 021211. Applying the above correction lowers the estimated position of the GRB on the light of this host from the 75.8 to the 75.0 percentile. This is not large enough to cause GRB 021211 to change its position in relation to the SN hosts, nor do any of the GRB hosts above 021211 now fall below it. Thus our conclusion that the SN and GRB hosts populations are not drawn from the same distribution is entirely unaffected. While the comparison of the GRB sample with the analytical model of objects tracing light changes slightly, the probability that the GRBs do follow the light of their hosts remains insignificant.

2 Supplementary Notes

Additional Comment on Sample Bias: LGRB redshifts are generally obtained through spectroscopy. It is rare that a LGRB or its host have sufficient colors to allow the determination of a photometric redshift. Only a fraction of LGRB spectroscopic redshifts have been obtained through absorption lines imposed upon the OT light by the host. Nearly half of redshifts have been obtained by emission lines seen from the host. This means that the sample of LGRBs with known redshifts is biased towards bright hosts. Indeed we know of three GRBs (980326[3], 020410[4], and 030723[5]), which have apparent supernova "bumps" in their light curves indicating a redshift $\lesssim 1$, but which have no measured redshift. At the same time only one potential core-collapse supernova (cc SN) in the GOODs sample does not have a spectroscopic or photometric redshift. Thus our sample almost certainly understates the true differences in magnitude and size between the LGRB and cc SN hosts.

For consistency, we have used *HST* optical magnitudes where possible. The bands used typically correspond to the far blue or ultraviolet in the host rest frame. This is entirely appropriate for the study of the location of the explosions on their hosts, as these positions are expected to be correlated with star-formation and thus blue or ultraviolet light; however, redder observing bands (for which the data are less complete for the GRB hosts) would better correlate with host mass. Given the difference in host morphology observed between the GRB and SN hosts, it is likely that a comparison in redder bands would accentuate the already strong difference in host magnitudes seen between these two samples.

Finally, LGRBs usually (though not always) begin their lives with optical afterglows that are dramatically brighter than their hosts. (Furthermore, LGRBs often have x-ray or radio afterglows which can be used to identify a host.) SNe often do not dominate their host, and thus one might worry that some SNe may have been missed by the GOODS group, particularly in the cores of galaxies, where subtraction errors are greatest, and the contrast with the host the poorest. To test this possibility we have compared the brightness of the cc SNe with the subtraction errors at the cores of their hosts (images at each epoch are subtracted from a template in order to discover the SNe). We find that for 15 of the 16 objects, the cc SNe were clearly brighter at observed peak than the largest errors on their hosts and would have been easily detected. Only in the case of 2002ke were the errors in three central pixels large enough to compromise the discovery of the SN. We therefore estimate that less than $\sim 10\%$ of central SNe were missed by the GOODS search.

A referee noted that the SN hosts tend more toward face-on than edge-on and this could be due to a failure to detect SNe in edge on spirals potentially because of a large line-of-sight through a dusty galaxy. Indeed, there may be such a selection effect for SNe (this should be less of a problem for GRBs, primarily because GRBs can also be detected in the radio and X-ray, but also because GRBs may be able to destroy dust along significant path-lengths [6,7]). However, as the effect of orientation is likely to be more pronounced in spirals than in irregulars, this effect would tend to suppress the number of spirals relative to irregulars in the SN sample. Thus such a loss of SNe would probably tend to reduce the number of spirals in the GOODS sample, and the true differences between the SN and GRB hosts could be even larger than reported here.

3 Supplementary Tables

In the tables below we present further information on the observations used to derive the results in the accompanying paper.

In Tables 1-3 we provide details of the GRB observations. We present the *HST* instrument used, the observed host magnitude, the redshift of the GRB (where known) the derived host absolute magnitude (including an estimated correction for foreground Galactic extinction), a radius estimated to enclose 80% of the host light, the fractional light of the host contained in pixels fainter than or equal to that at the position of the GRB, and our estimated positional uncertainty in the GRB. Magnitudes for all objects were obtained from *HST* imaging except in the case of GRBs 980425[8], 000210[9], 000911[10], 020819[11], and 031203[12] where ground based magnitudes are used. All STIS observations are through the "CLEAR" filter; all ACS observations are with the F606W filter; all WFPC2 observations are with the F555W filter except for GRBs 040924 and 041106 which were observed with the F775W filter, and GRB 000131 for which the F814W filter was used. With the exceptions of GRBs 040924[13] and 041006[14], references for all GRB redshifts shown here can be found in Ref. 15. Only GRBs with relative astrometry better than $0\farcs15$ have their positional errors or fractional light levels shown. Fractional light levels are left blank in several other cases where our estimates suggested that the GRB OT might still contaminate the light of the host as described above. Host magnitudes were adjusted for foreground Galactic extinction based on the correction scheme given in Ref. 16.

In Table 4 we present the observed properties of the GOODS SNE hosts. The redshifts for

these objects are as determined in Ref. 17. The size, magnitude, and position determinations shown here were performed in an identical manner to those for the GRB hosts.

In Table 5 we present a short table of observations in cases where a ground-based image was used to determine the position of a GRB on a host. In addition to these observations, two positions were obtained from the literature – GRB 971214 from Ref. 18 and GRB 980613 from Ref. 19. Both ground-based and early *HST* images were aligned to late-time *HST* images using fits for the positions of objects which were unresolved or only marginally resolved in the *HST* images. When ground-based images were aligned to an *HST* image a fit for scale, rotation and translation was done. When *HST* images were aligned, the fit was for rotation and translation only. The *HST* images used in this program are all available from the *HST* public archive: http://archive.stsci.edu.

Table 1 GRB Host Galaxies: 1997-1999

GRB	INST	Mag(AB)	z	M_V	r_{80}(kpc)	F_{light}	P_{err} (")
970228	STIS	25.88	0.685	-17.26	3.2	-	0.025
970508	STIS	25.19	0.84	-17.92	1.48	100	0.007
970828	WFPC2	24.43	0.958	-18.93	2.8	-	-
971214	STIS	26.35	3.42	-20.49	2.36	53.5	0.150
980326	STIS	29.73	1	-13.85	-	100	0.033
980329	STIS	27.25	-	-	-	79.40	0.04
980425	GROUND	15.19	0.0085	-17.59	-	-	-
980519	STIS	28.09	-	-	-	84.83	0.05
980613	STIS	25.33	1.10	-18.48	3.75	41.6	0.075
980703	STIS	22.91	0.97	-20.55	2.42	55.7	0.035
981226	STIS	25.04	-	-	-	-	-
990123	STIS	24.41	1.60	-20.07	5.01	11.3	0.005
990506	STIS	25.53	1.30	-18.56	1.53	-	-
990510	STIS	28.20	1.62	-16.75	1.75	79.4	0.006
990705	STIS	22.78	0.86	-20.47	9.38	-	0.028
990712	STIS	22.45	0.43	-19.12	2.25	97.1	0.012
991208	STIS	24.60	0.71	-18.05	1.16	94.0	0.073
991216	STIS	26.79	1.02	-18.40	2.25	82.5	0.030

Table 2 GRB Host Galaxies: 2000-2001

GRB	INST	Mag(AB)	z	M_V	r_{80}(kpc)	F_{light}	P_{err} (")
000131	WFPC2	24.86	4.50	-21.50	5.93	49.1	0.100
000210	GROUND	24.22	0.85	-18.83	-	-	-
000301	STIS	28.90	2.03	-16.07	1.00	51.2	0.006
000418	STIS	24.15	1.12	-19.55	1.70	45.4	0.150
000911	GROUND	-	1.06	-18.95	-	-	-
000926	WFPC2	24.18	2.04	-20.73	10.25	100	0.013
010222	WFPC2	25.61	1.47	-18.62	2.87	92.7	0.013
010921	WFPC2	22.58	0.45	-19.41	2.76	43.9	0.015
011030	STIS	25.75	-	-	-	-	-
011121	WFPC2	23.23	0.36	-19.41	5.89	51.1	0.016
011211	STIS	25.97	2.12	-19.05	2.69	95.3	0.006

Table 3 GRB Host Galaxies: 2002-2004

GRB	INST	Mag(AB)	z	M_V	r_{80}(kpc)	F_{light}	P_{err} (")
020305	STIS	25.23	-	-	-	91.1	0.006
020322	STIS	26.50	-	-	-	28.2	0.090
020331	STIS	25.86	-	-	-	100	0.007
020405	WFPC2	21.59	0.69	-21.11	11.96	58.7	0.010
020410	STIS	27.26	-	-	-	97.3	0.006
020427	STIS	24.61	-	-	-	-	-
020813	ACS	24.46	1.25	-19.69	2.13	88.0	0.008
020819	GROUND	19.48	0.41	-21.88	-	-	-
020903	ACS	21.63	0.25	-18.98	1.43	95.8	0.006
021004	ACS	24.63	2.33	-20.63	1.81	100	0.006
021211	ACS	25.43	1.02	-18.05	1.63	75.8	0.007
030115	ACS	25.58	2.5	-	-	86.3	0.060
030323	ACS	27.28	3.37	-18.53	1.86	86.2	0.060
030329	ACS	23.07	0.17	-16.37	1.03	99.1	0.006
031203	GROUND	-	0.105	-20.73	-	-	-
040924	ACS	23.93	0.859	-19.21	3.234	-	0.013
041006	ACS	25.15	0.716	-17.53	5.19	-	0.008

Table 4 cc SNe in the GOODS survey

SNe	Mag(AB)	z	M_V	r_{80}(kpc)	F_{light}
2002fz	22.34	0.84	-20.64	11.70	59.2
2002hq	20.93	0.67	-21.54	16.60	37.1
2002hs	23.25	0.90	-19.87	12.75	9.3
2002kb	20.54	0.58	-21.61	15.82	83.7
2002ke	21.05	0.58	-21.10	18.17	44.2
2002kl	22.54	0.41	-18.82	5.91	13.6
2003N	24.61	0.43	-17.09	3.73	69.1
2003ba	19.92	0.29	-20.65	8.181	81.6
2003bb	21.53	0.95	-21.72	20.37	17.8
2003bc	21.77	0.51	-20.09	4.450	19.9
2003dx	23.26	0.46	-18.36	2.167	44.9
2003dz	25.67	0.48	-16.18	2.47	61.0
2003ea	24.01	0.89	-19.42	4.38	56.7
2003er	21.24	0.63	-19.70	7.16	8.4
2003et	22.98	0.83	-19.79	4.97	85.9
2003ew	21.97	0.66	-20.10	15.21	71.4

Table 5 Ground-based Astrometric Observations

GRB	Tel Inst	Date
980326	Keck/LRIS	1998-03-27
980329	Calar Alto 3.5m	1998-03-29
980519	INT/WFC	1998-05-20
980703	NTT/EMMI	1998-07-04
990705	NTT/SOFI	1999-07-05
991208	NOT/StanCam	1999-12-12
991216	VLT/FORS	1999-12-18
000131	VLT/FORS	2002-02-04
020322	PAL-60	2002-03-22
030115	VLT/ISAAC	2003-01-17

4 Supplementary Figures

In Supplementary Figures 1–3 we show *HST* images of all of the host galaxies used in the position study. Each galaxy is shown as a pair of images. The left-hand image of each pair shows the pixels which were determined by Sextractor to lie above the signal-to-noise cut. The right-hand image shows the *HST* image with a small green circle centered on the position of the GRB.

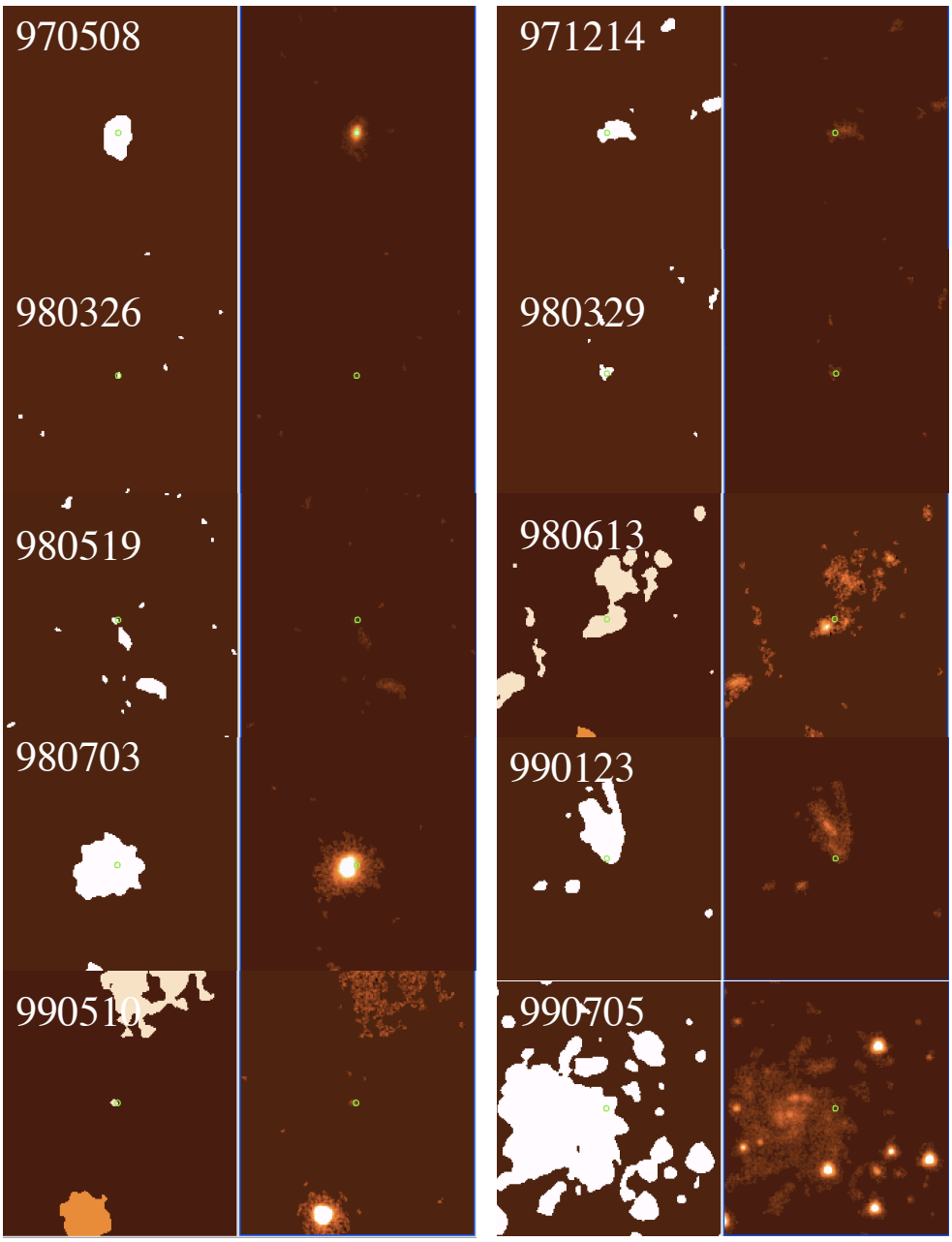
970508
971214
980326
980329
980519
980613
980703
990123
990510
990705

Figure 1

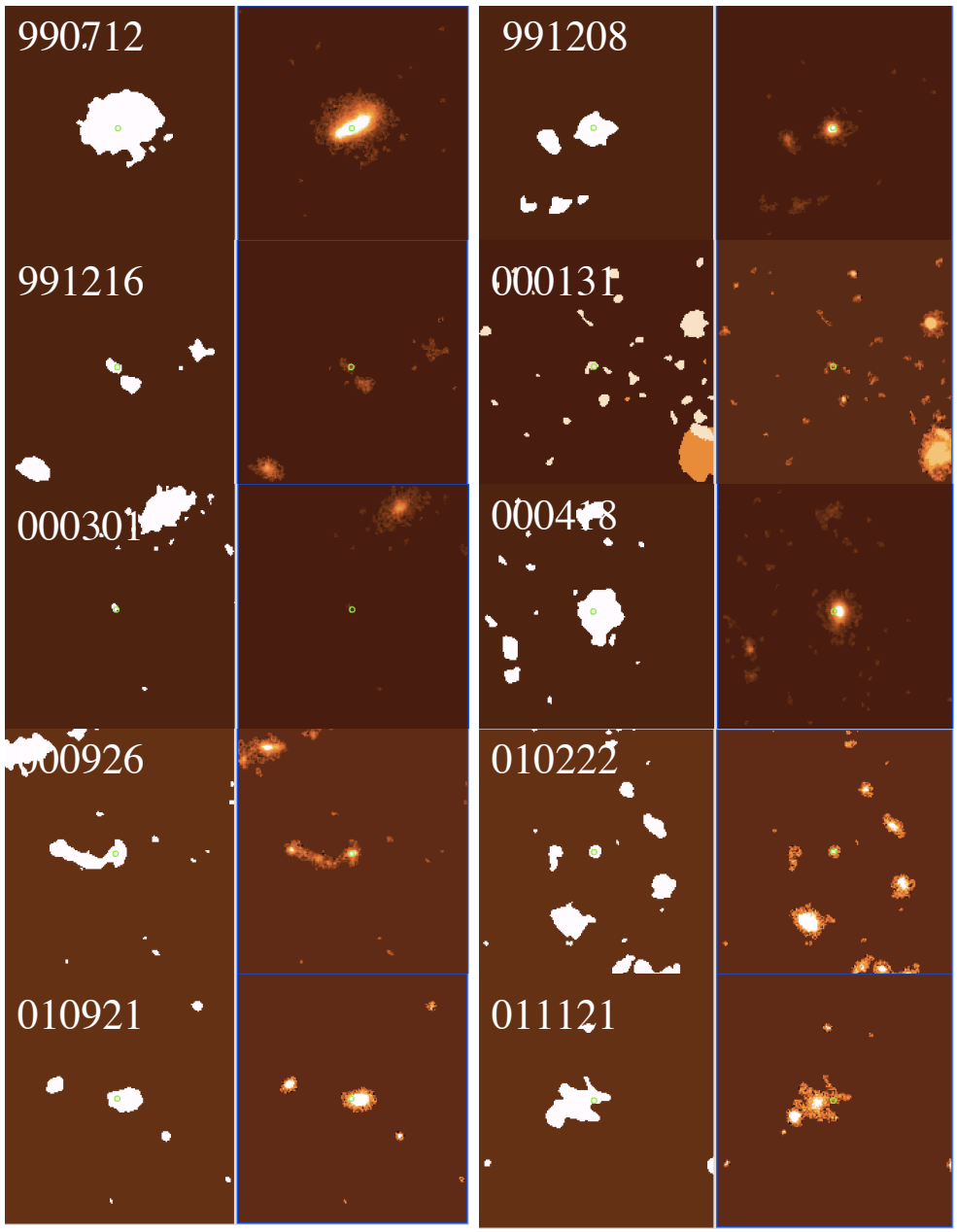
990712
991208
991216
000131
000301
000418
000926
010222
010921
011121

Figure 2

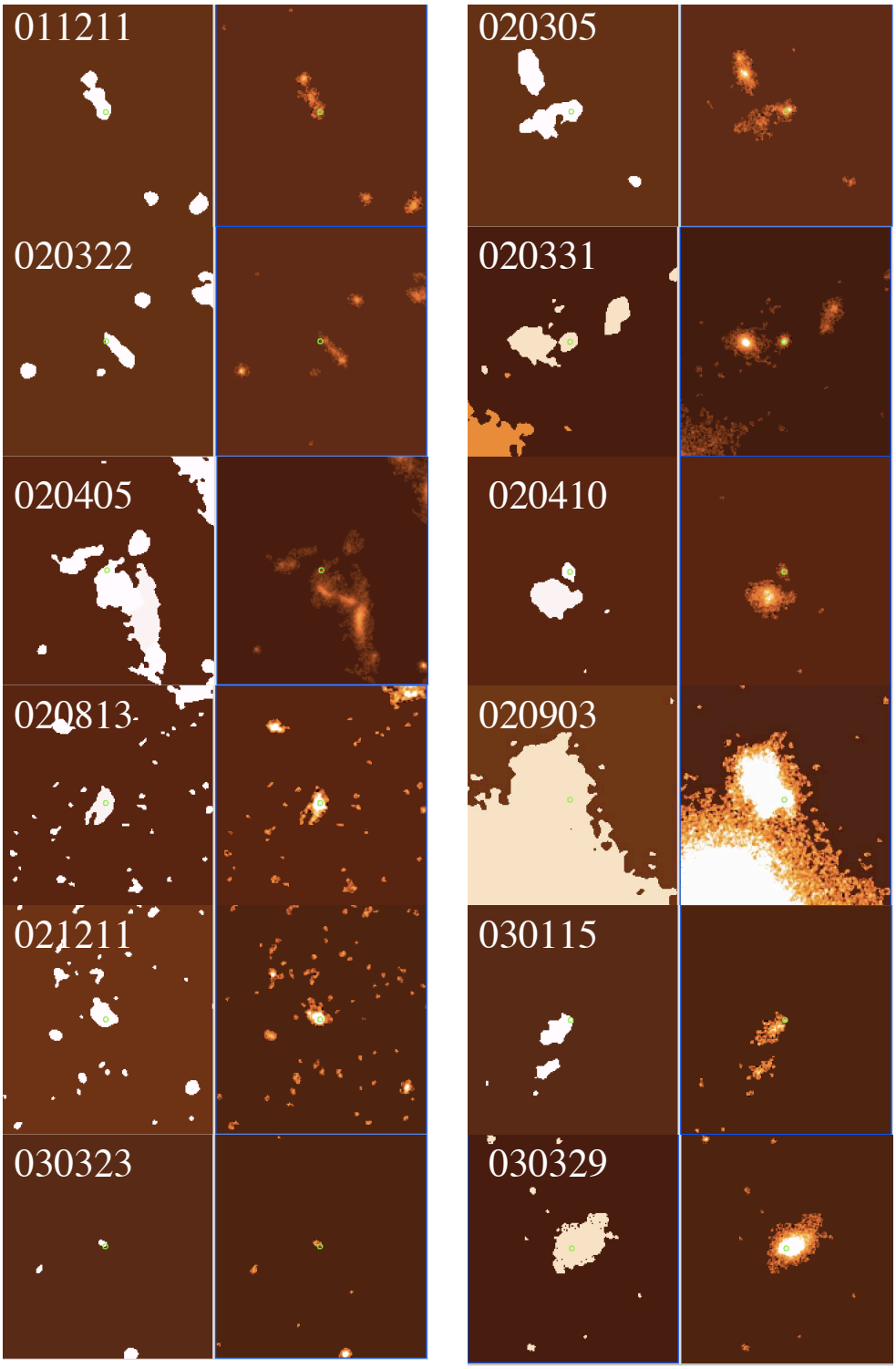
011211
020305
020322
020331
020405
020410
020813
020903
021211
030115
030323
030329

Figure 3

5 References for Supplementary Material

1. Bertin, E. & Arnouts, S. SExtractor: Software for source extraction. *Astr. Astrophys. Suppl. Ser.* **117**, 393–404 (1996).

2. Fruchter, A. S. & Hook, R. N. Drizzle: A Method for the Linear Reconstruction of Undersampled Images. *Publ. Astr. Soc. Pacific* **114**, 144–152 (2002).

3. Bloom, J. S. *et al.* The unusual afterglow of the gamma-ray burst of 26 March 1998 as evidence for a supernova connection. *Nature* **401**, 453–456 (1999).

4. Levan, A. *et al.* GRB 020410: A Gamma-Ray Burst Afterglow Discovered by Its Supernova Light. *Astrophys. J.* **624**, 880–888 (2005).

5. Fynbo, J. P. U. *et al.* On the Afterglow of the X-Ray Flash of 2003 July 23: Photometric Evidence for an Off-Axis Gamma-Ray Burst with an Associated Supernova? *Astrophys. J.* **609**, 962–971 (2004).

6. Waxman, E. & Draine, B. T. Dust Sublimation by Gamma-ray Bursts and Its Implications. *Astrophys. J.* **537**, 796–802 (2000).

7. Fruchter, A., Krolik, J. H. & Rhoads, J. E. X-Ray Destruction of Dust along the Line of Sight to γ-Ray Bursts. *Astrophys. J.* **563**, 597–610 (2001).

8. Fynbo, J. U. *et al.* Hubble Space Telescope Space Telescope Imaging Spectrograph Imaging of the Host Galaxy of GRB 980425/SN 1998BW. *Astrophys. J.* **542**, L89–L93 (2000).

9. Gorosabel, J. *et al.* A multi-colour study of the dark GRB 000210 host galaxy and its environment. *Astr. Astrophys.* **400**, 127–136 (2003).

10. Masetti, N. *et al.* Late-epoch optical and near-infrared observations of the GRB 000911 afterglow and its host galaxy. *Astr. Astrophys.* **438**, 841–853 (2005).

11. Jakobsson, P. *et al.* The Radio Afterglow and Host Galaxy of the Dark GRB 020819. *Astrophys. J.* **629**, 45–51 (2005).

12. Malesani, D. *et al.* SN 2003lw and GRB 031203: A Bright Supernova for a Faint Gamma-Ray Burst. *Astrophys. J.* **609**, L5–L8 (2004).

13. Wiersema, K., Starling, R. L. C., Rol, E., Vreeswijk, P. & Wijers, R. A. M. J. GRB 040924: VLT spectroscopy. *GRB Circular Network* **2800** (2004).

14. Soderberg, A. M. *et al.* An HST Study of the Supernovae Accompanying GRB040924 and GRB041006. *Astrophys. J.* (2005). Submitted, astro-ph/0504359.

15. Conselice, C. J. *et al.* Gamma-Ray Burst Selected High Redshift Galaxies: Comparison to Field Galaxy Populations to z˜3. *Astrophys. J.* **633**, 29–40 (2005).

16. Schlegel, D. J., Finkbeiner, D. P. & Davis, M. Maps of dust infrared emission for use in estimation of reddening and cosmic microwave background radiation foregrounds. *Astrophys. J.* **500**, 525–553 (1998).

17. Strolger, L.-G. *et al.* The Hubble Higher z Supernova Search: Supernovae to z ˜ 1.6 and Constraints on Type Ia Progenitor Models. *Astrophys. J.* **613**, 200–223 (2004).

18. Odewahn, S. C. *et al.* The host galaxy of the gamma-ray burst 971214. *Astrophys. J.* **509**, L5–L8 (1998).

19. Holland, S. HST/STIS observations of the chaotic environment of GRB 980613. *GRB Coordinates Network* **777**, 1 (2000).